

Sunlight Photolysis of Safener Benoxacor and Herbicide Metolachlor as Mixtures on Simulated Soil Surfaces

Lei Su,[†] Leandra M. Caywood,[‡] John D. Sivey,[§] and Ning Dai^{*,†} 

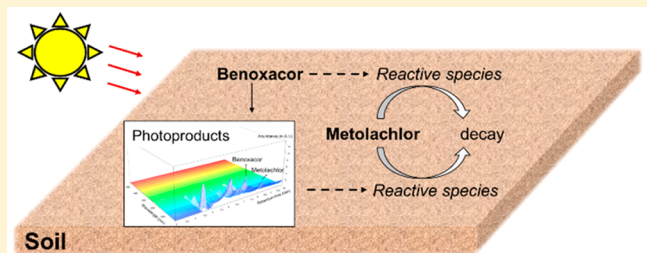
[†]Department of Civil, Structural and Environmental Engineering, University at Buffalo, The State University of New York, Buffalo, New York 14260, United States

[‡]Department of Chemical and Materials Engineering, University of Alabama in Huntsville, Huntsville, Alabama 35899, United States

[§]Department of Chemistry, Towson University, Towson, Maryland 21252, United States

Supporting Information

ABSTRACT: Benoxacor is a safener paired with the high-use herbicide S-metolachlor. Commercial formulations containing both compounds are sprayed onto soil pre-emergence to enhance yields of corn. In this study, we evaluated the sunlight photolysis of metolachlor and benoxacor, individually and as mixtures, in three different reaction environments: in water and on two soil-simulating surfaces (quartz and kaolinite). When irradiated individually, benoxacor degraded at least 19 times faster than metolachlor in each reaction environment, consistent with its higher molar absorptivity within the solar spectrum than metolachlor. When metolachlor and benoxacor were irradiated as mixtures, benoxacor promoted metolachlor degradation on quartz and, to a lesser extent, in water, but not on kaolinite. On quartz, at a benoxacor/metolachlor molar ratio of 0.1:1, metolachlor degraded 1.8 times faster than in the absence of benoxacor; as the benoxacor/metolachlor ratio increased, metolachlor degradation rate also increased. The photolysis rate of benoxacor depended on its initial surface concentration and was promoted by metolachlor. Benoxacor photoproducts were capable of absorbing sunlight and serving as photosensitizers for metolachlor degradation. These results illustrate how a safener can influence the photochemistry of its coformulated herbicide and suggest that such mixture effects should be considered when evaluating the environmental fate of agrochemicals.



1. INTRODUCTION

Sunlight photolysis is an important transformation process for many herbicides. In addition to contributing to their degradation in aqueous environments,^{1–3} direct and indirect photolysis can also transform herbicides on soil surfaces.^{4–6} Because of the low light penetration into soil,^{7,8} direct photolysis is typically limited to the top 0.4 mm of soil.^{8–12} In comparison, indirect photolysis can be more prevalent as reactive intermediates diffuse further into the soil.^{9,12} Typical soil has abundant photosensitizers, including minerals^{13,14} and natural organic matter,^{15,16} which can form reactive species such as singlet oxygen ($^1\text{O}_2$)^{6,17–19} and hydroxyl radical ($\bullet\text{OH}$).^{6,13} These reactive species were shown to promote contaminant degradation on soil surfaces.^{13,19}

Commercial herbicide formulations often contain adjuvants that enhance the performance of the active ingredient(s).²⁰ Different herbicides can also be applied simultaneously. The behavior of photoreactive herbicides and adjuvants on environmental surfaces can vary depending on whether they are applied individually or as mixtures. For example, when two commercial herbicides (mesotrione and nicosulfuron) were coapplied on maize wax surface, their photodegradation rates were 1.5 and 2.3 times higher, respectively, than when they were applied individually.²¹ Similarly, the herbicide cycloxydim photodegraded three times faster on wax when coapplied with

similar amounts of the fungicide chlorothalonil.²² Conversely, the presence of grape extract as a coformulant decreased the direct photolysis rates of five pesticides on carnauba gray wax surface by 38–72%.²³

Safeners are a group of adjuvants that can selectively protect crop plants from active herbicidal ingredients.²⁴ Benoxacor is a dichloroacetamide safener and is paired with the herbicide S-metolachlor. S-Metolachlor is one of the most used herbicides in the U.S.,²⁵ with an estimated application of 2.3×10^7 kilograms in 2015.²⁶ The commercial formulations use benoxacor-to-S-metolachlor molar ratios ranging from 0.05:1 to 0.14:1^{27–30} and are recommended for pre-emergent application (i.e., spraying onto soil).^{31,32} Metolachlor has four stereoisomers with both S- and R- enantiomers existing as pairs of atropisomers.³³ Regardless of the isomeric form, direct photolysis of metolachlor in water is slow (half-life 4–8 days).^{34,35} Benoxacor, in contrast, exhibits a broad UV absorbance band overlapping with the sunlight spectrum²⁷ and therefore is likely to undergo direct photolysis.

Received: February 27, 2019

Revised: May 19, 2019

Accepted: May 27, 2019

Published: May 27, 2019

Despite the widespread global use of herbicide + safener formulations,²⁷ potential interactions between photoreactive safeners and the corresponding herbicides have not been studied on environmental surfaces. Investigations of possible herbicide-safener photochemical interactions in solution showed no mixture effects for the metolachlor-benoxacor pair in water³⁶ nor for the herbicide *S*-ethyl-*N,N*-dipropylthiocarbamate and its safener dichlormid in methanol or water.³⁷ However, photolysis rates and pathways on surfaces can differ significantly from that in the bulk solutions. For example, the direct photolysis of 2,4-D herbicides on quartz was 85–245 times faster than that in methanol; moreover, photolysis on quartz proceeded through unique pathways not observed in methanol.³⁸ Additionally, in contrast to the relatively low concentrations of herbicides and safeners in surface water proximate to agricultural lands (ng/L levels),³⁹ their concentrations on soil surface after initial application are on the order of 1.5–15 $\mu\text{g cm}^{-2}$ (5×10^{-3} – 5×10^{-2} $\mu\text{mol cm}^{-2}$),³¹ suggesting a higher probability of mixture effects during photolysis.

The aim of the present work is to evaluate the interaction between the safener benoxacor and the herbicide metolachlor in their photodegradation on model soil surfaces. First, the direct photolysis rate constants for benoxacor and metolachlor were determined in three different reaction environments: in water, on quartz, and on kaolinite. Quartz and kaolinite were selected as model surfaces for soil.^{4,40,41} Subsequently, the photolysis of benoxacor and metolachlor was evaluated when applied as mixtures with varying benoxacor-to-metolachlor ratios in all three reaction environments. Lastly, ultraviolet–visible absorption spectrum and high-resolution mass spectrometry analyses were conducted to characterize the photoproducts.

2. MATERIALS AND METHODS

2.1. Chemicals. Detailed information on the chemicals used in this study is shown in *Text S1 in the Supporting Information (SI)*. The metolachlor obtained from Sigma-Aldrich contained >60% *S*-metolachlor.

2.2. Photolysis Experiments. Stock solutions of metolachlor and benoxacor were prepared in acetonitrile. The sample preparation procedure for experiments in water is described in *SI Text S2 and Table S1*. For surface experiments, quartz dishes (diameter 55 mm, depth 15 mm, capacity 20 mL) served as the quartz surface. Before experiments, the quartz dishes were thoroughly rinsed by deionized water, wrapped in aluminum foil, and baked in the oven at 450 °C for 3 h. The preparation of kaolinite surface followed a published procedure¹³ and is described in *SI Text S3*. The thickness of kaolinite layer used in our experiments was estimated to be 0.08 mm. Solutions of metolachlor, benoxacor, or their mixtures were deposited on quartz or kaolinite surfaces in 10 evenly spaced microdroplets (10 μL each). The surfaces were stored in the dark for 0.5 h to allow the solvent (acetonitrile) to evaporate. During this process, dishes were placed under a box cover to minimize the deposition of indoor dust on the surfaces. During preparation of surface samples, a sodium lamp ($\lambda = 589$ nm) was used for laboratory illumination to minimize unintentional photolysis. The initial concentrations of metolachlor and benoxacor on surfaces are shown in *SI Table S2*. The initial surface concentrations (4.8×10^{-4} – 1.0×10^{-2} $\mu\text{mol cm}^{-2}$) were lower than typical field applications (1.5 L ha^{-1} , equivalent to 4.8×10^{-2} $\mu\text{mol cm}^{-2}$)³¹ due to the

limits of microdroplet volume on surfaces and compound solubility in acetonitrile. Sample irradiation was conducted in a Q-SUN Xe-1 test chamber equipped with a Xenon arc lamp to produce the full sunlight spectrum. Details of the test chamber and sample irradiation procedure are provided in *SI Text S4*. All experiments were conducted in triplicate and included dark control samples.

2.3. Analysis of Metolachlor and Benoxacor Degradation. The degradation of metolachlor and benoxacor in aqueous samples was analyzed by high-performance liquid chromatography with a diode array detector (HPLC-DAD). Quartz surface samples were extracted by 5 mL acetonitrile and analyzed by HPLC-DAD. For kaolinite surface samples, 10 mL acetonitrile were added to create a kaolinite slurry, and the slurry was scraped off by a spatula and transferred to a 50 mL centrifuge tube. The tube was placed on an orbital shaker for 20 min, and then centrifuged for 10 min at 4000 rpm and 23 °C. The supernatant was filtered by a 0.45 μm glass fiber filter and analyzed by HPLC-DAD. The recoveries of metolachlor and benoxacor from the two surfaces were 82.8–110.9% (*SI Table S3*). For samples with a 0.1:1 benoxacor-to-metolachlor molar ratio in water and on quartz, benoxacor concentration was quantified by an LC triple quadrupole mass spectrometer (LC-QQQ) to achieve a lower detection limit. Additional details on the HPLC-DAD and LC-QQQ methods are provided in *SI Text S5*.

2.4. Analysis of the Sunlight Absorption Ability and Photoproducts of the Irradiated Samples. Aqueous and quartz surface samples featuring an initial 10:1 benoxacor/metolachlor molar ratio were analyzed for their photoproducts. First, the 200–800 nm absorption spectra (corrected against a solvent blank) were measured by a UV–vis spectrophotometer (Agilent Cary 60) for the irradiated mixtures collected at selected time points. Water samples were analyzed directly. Quartz surface samples were extracted by 5 mL acetonitrile, and the extracts were analyzed. The sunlight absorption ability of the samples, $W(t)$, in units of Einstein $\text{cm}^{-2} \text{ s}^{-1}$, was calculated by *eq 1*:

$$W(t) = \sum_{\lambda} E_p^0(\lambda)(1 - 10^{-a(\lambda)t})\Delta\lambda \quad (1)$$

where t is the irradiation time (h); $E_p^0(\lambda)$ is the incident light intensity (Einstein $\text{cm}^{-2} \text{ s}^{-1} \text{ nm}^{-1}$) at wavelength λ (nm); $a(\lambda)t$ is the absorbance coefficient (cm^{-1}) of the sample (aqueous or acetonitrile extracted) collected at time t at wavelength λ ; and l is the sample path length (cm). The $a(\lambda)t$ exponent for surface samples was approximated by that of the acetonitrile extract (see *SI Text S6* for additional discussion). Second, the aqueous samples and the acetonitrile extracts of surface samples were analyzed by HPLC-DAD (*SI Text S5*) to explore light-absorbing photoproducts and to evaluate their polarity compared with the parent compounds based on relative retention times. Third, samples were analyzed using ultra performance liquid chromatography interfaced with a quadrupole/time-of-flight mass spectrometer using an electrospray ionization source (operated in positive ionization mode) (UPLC-ESI(+)-qTOF). Product identification was based on accurate mass measurements. Details of the UPLC-ESI(+)-qTOF method are shown in *SI Text S5*.

3. RESULTS AND DISCUSSION

3.1. Direct Photolysis of Metolachlor and Benoxacor. *Figure 1A* shows the time profile of metolachlor concentrations

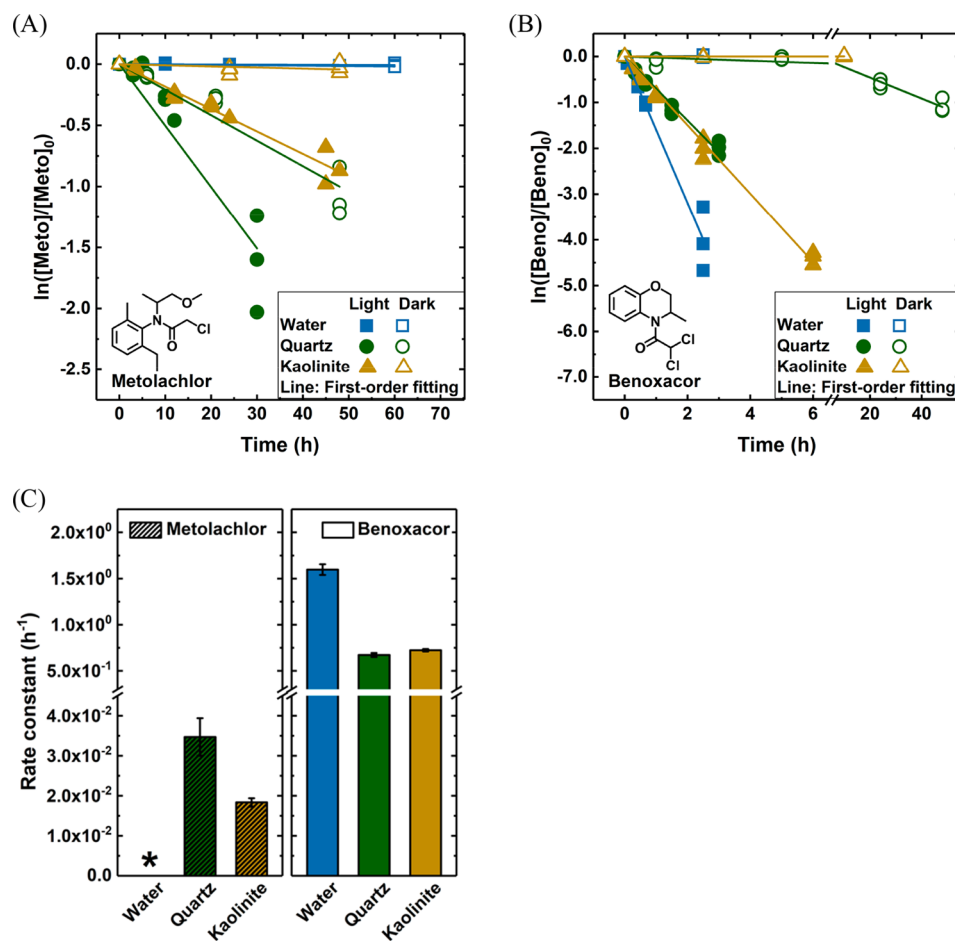


Figure 1. Photodegradation of (A) metolachlor and (B) benoxacor individually in water and on quartz and kaolinite surfaces. (C) Pseudo-first-order photolysis rate constants of metolachlor and benoxacor. Error bars represent the standard error of triplicate experiments (SI Text S9). Simulated sunlight 320 W m^{-2} as determined by actinometer 2-NB; 26°C ; aqueous sample pH 7 (5 mM phosphate buffer). The initial concentrations of metolachlor and benoxacor are summarized in SI Tables S1 and S2. *No degradation of metolachlor was observed over 60 h in water. Beno = benoxacor; Meto = metolachlor.

in irradiated and dark control samples. In water, metolachlor showed no discernible photodegradation over 60 h, suggesting a rate constant smaller than $9 \times 10^{-4} \text{ h}^{-1}$. On kaolinite surface, metolachlor photolysis followed pseudo-first-order kinetics, with a rate constant of $(1.8 \pm 0.1) \times 10^{-2} \text{ h}^{-1}$ (mean \pm standard error, same below). On quartz surface, loss of metolachlor was observed in the dark, but it did not account for the majority of the loss in irradiated samples. Because pseudo-first-order kinetics were observed in both irradiated and dark control samples, the photolysis rate constant on quartz (k_{photo}) was calculated as eq 2.

$$k_{\text{photo}} = k_{\text{obs}} - k_{\text{dark}} \quad (2)$$

where k_{obs} and k_{dark} are the rate constants (h^{-1}) for the loss of metolachlor in irradiated and dark control samples, respectively. This yielded the photolysis rate constant for metolachlor on quartz $(3.5 \pm 0.5) \times 10^{-2} \text{ h}^{-1}$. The loss of metolachlor from quartz surface in the dark was likely due to volatilization (see SI Text S7 for further discussion).

This is the first report of metolachlor photolysis on quartz and kaolinite surfaces. The rate constants for these two surfaces were within a factor of 2 (Figure 1C). Although kaolinite was previously shown to participate in photochemical reactions by generating $\bullet\text{OH}$ ¹³ while quartz is considered an inert surface, metolachlor photolysis on kaolinite was slower

than on quartz. Therefore, any additional contribution of $\bullet\text{OH}$ was seemingly offset by the reduced light exposure within the kaolinite layer. The photodegradation of metolachlor on surfaces contrasted its recalcitrance toward photolysis in aqueous solution. Previous studies showed that the absorption spectra of organic compounds on surfaces can experience bathochromic shifts compared with their absorption spectra in water due to compound-compound as well as compound-surface interactions.^{42–44} Such shifts could increase the ability of sorbates to absorb sunlight and to thereby undergo direct photolysis. SI Figure S1B shows the absorption spectrum of metolachlor on quartz, which indeed has a greater overlap with the sunlight spectrum compared with its absorption spectrum in water. Our measurements were not, however, able to yield a molar extinction coefficient. Future work should include further characterization based on diffuse reflectance spectroscopy.⁴² The lack of metolachlor photolysis in water ($<9 \times 10^{-4} \text{ h}^{-1}$) in this study (light intensity 320 W m^{-2}) contradicts the previously reported rate constants $8.0 \times 10^{-3} \text{ h}^{-1}$ and $9.5 \times 10^{-3} \text{ h}^{-1}$ under light intensities of 750 W m^{-2} and 765 W m^{-2} , respectively.^{34,35} Since the absorbance spectrum of metolachlor in water under our experimental conditions (buffered at pH 7 by phosphates) did not overlap with the simulated sunlight spectrum (SI Figure S1A), direct photolysis of metolachlor is unlikely. The observed degradation in previous studies may be

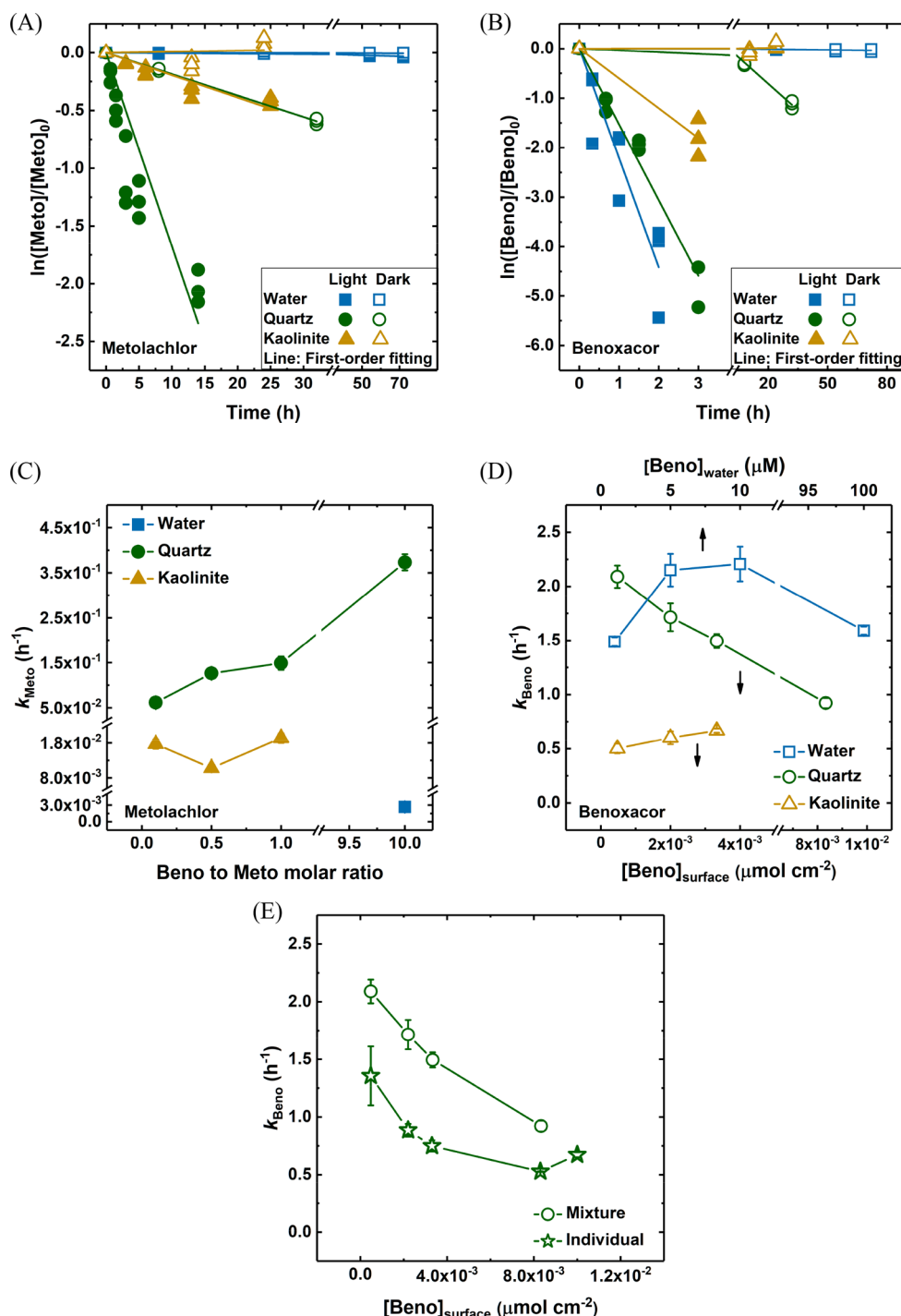


Figure 2. Time profiles of (A) metolachlor and (B) benoxacor degradation in mixtures with a 1:1 initial benoxacor/metolachlor molar ratio. Pseudo-first-order photolysis rate constants of (C) metolachlor and (D) benoxacor in mixtures with varying initial benoxacor/metolachlor molar ratios. (E) Comparison of benoxacor photolysis rate constants on quartz when applied at different initial concentrations individually or as benoxacor/metolachlor mixtures. Error bars represent the standard error of triplicate experiments (SI Text S9). Simulated sunlight 320 W m⁻² as determined by actinometer 2-NB; 26 °C. The initial concentrations of metolachlor and benoxacor are summarized in SI Tables S1 and S2. Metolachlor degradation was not observed in water after 72 h for mixtures with 0.1:1, 0.5:1, and 1:1 benoxacor/metolachlor ratios. The 10:1 benoxacor/metolachlor ratio was not evaluated on kaolinite surface. Beno = benoxacor; Meto = metolachlor.

attributed to the more acidic pH (5.35)³⁴ or unbuffered reaction solution³⁵ and higher light intensity.

Figure 1B shows the time profile of benoxacor concentrations in irradiated and dark control samples. In all reaction media, benoxacor photolysis followed pseudo-first-order kinetics. The rate constants in water and on kaolinite surface

were 1.6 ± 0.06 and 0.72 ± 0.01 h⁻¹, respectively; the rate constant on quartz, after accounting for the loss in the dark (SI Text S7), was 0.67 ± 0.02 h⁻¹. Benoxacor photolysis was at least 19 times faster than metolachlor in the same reaction environment (Figure 1C), consistent with its higher molar absorptivity within the sunlight region of 290–350 nm (SI

Figure S1A). The quantum yield of benoxacor photolysis in water was determined to be 6.1×10^{-2} (see SI Text S8 for calculation method), somewhat lower than a recently reported value (1.4×10^{-1}).³⁶ This difference may be attributed to the usage of different chemical actinometers, 2-NB in the present study versus the para-nitroanisole/pyridine actinometer system in the previous study.

3.2. Photolysis of Benoxacor/Metolachlor Mixtures.

Figure 2A,B and SI Figure S2 show the time profile of metolachlor and benoxacor degradation when they were applied as mixtures with varying benoxacor/metolachlor molar ratios. Dark control samples for quartz experiments again showed loss of parent compounds over time, but the associated rate constants did not show any dependence on the benoxacor/metolachlor ratios (SI Figure S3, Text S7).

On quartz, metolachlor degraded faster when coapplied with benoxacor than when it was applied individually; the higher the benoxacor/metolachlor ratio, the faster metolachlor degraded (Figure 2C). At the lowest benoxacor/metolachlor ratio tested (0.1:1), the rate constant of metolachlor ($6.2 \pm 0.6 \times 10^{-2} \text{ h}^{-1}$) was 1.8 times higher than in the absence of benoxacor ($3.5 \pm 0.5 \times 10^{-2} \text{ h}^{-1}$). Considering that benoxacor more strongly absorbs sunlight than metolachlor, if the photosensitizing effect were absent, light shielding by benoxacor should slow down metolachlor photolysis. Therefore, with the observed trend, photosensitization likely contributed to metolachlor decay. In water, metolachlor photodegradation remained undetectable across benoxacor/metolachlor molar ratios from 0.1:1 to 1:1; in the mixture with 10-fold excess of benoxacor, photodegradation of metolachlor was detected but slow, with a rate constant of $(2.6 \pm 0.3) \times 10^{-3} \text{ h}^{-1}$. On kaolinite, degradation of metolachlor in mixtures proceeded with similar rate constants (1.1×10^{-2} – $1.9 \times 10^{-2} \text{ h}^{-1}$) as in the absence of benoxacor ($1.8 \pm 0.1 \times 10^{-2} \text{ h}^{-1}$). These results suggest that benoxacor served as a photosensitizer for metolachlor photodegradation on quartz and, to a lesser extent, in water, but not on kaolinite. The absence of sensitized reaction on kaolinite may be attributed to the greater distance between metolachlor and benoxacor as a result of the larger specific surface area provided by kaolinite particles.^{45,46} The stronger sensitizing effect of benoxacor on quartz than in water was similar to that observed for phenol, furfuryl alcohol, tryptophan, and bisphenol A in ice, where sensitized reactions by excited triplet state 3,4-dimethoxybenzaldehyde and ${}^1\text{O}_2$ were more than 50 times faster than those in water.^{47,48} Two factors may have contributed to the stronger sensitizing effect on quartz: First, the half-life of reactive species such as $\bullet\text{OH}$ and ${}^1\text{O}_2$ are typically longer in air than in water.^{49,50} Second, metolachlor and benoxacor molecules were ostensibly in closer proximity on quartz, facilitating the interaction between metolachlor and the reactive species generated by benoxacor.

It was noteworthy that on quartz, metolachlor continued to decay after most benoxacor had degraded. For example, in the benoxacor/metolachlor 1:1 mixture, metolachlor degradation continued over 14 h, despite that >99% of benoxacor was degraded within the first 3 h (Figure 2A and B). Additionally, the decay profile of metolachlor showed deviation from pseudo-first-order kinetics (Figure 2A). In order to identify whether direct photolysis accounted for all of the metolachlor decay after nearly complete degradation of benoxacor, metolachlor's time profile data were fitted to pseudo-first-order kinetics in two consecutive time periods, with benoxacor surface concentration $2.5 \times 10^{-5} \mu\text{mol cm}^{-2}$ as the cutoff

(corresponding to HPLC detection limit $0.1 \mu\text{M}$ after extraction). SI Figure S4 is an example of the fitting and SI Table S4 shows the rate constants within each time period. With a low benoxacor/metolachlor ratio of 0.1:1, metolachlor degradation rate constant in the second time period ($(3.9 \pm 0.5) \times 10^{-2} \text{ h}^{-1}$) was similar to its direct photolysis ($(3.5 \pm 0.5) \times 10^{-2} \text{ h}^{-1}$). When the benoxacor/metolachlor ratios increased to 0.5:1 and 1:1, however, metolachlor degradation rate constants in the second time period ($(7.3 \times 10^{-2}$ – $1.0 \times 10^{-1} \text{ h}^{-1}$) were 2–3 times faster than its direct photolysis, suggesting that the photoproducts formed in the benoxacor/metolachlor mixtures can sensitize metolachlor degradation.

Because metolachlor has limited sunlight absorption, we first hypothesized that benoxacor photolysis in the mixtures was not affected by metolachlor. Accordingly, we plotted in Figure 2D the photolysis rate constant of benoxacor in mixtures as a function of its initial concentrations, rather than the benoxacor/metolachlor ratio. In water, the rate constants of benoxacor photolysis in mixtures were in the range of 1.5 – 2.2 h^{-1} (Figure 2D), similar to that when benoxacor was irradiated alone ($1.6 \pm 0.06 \text{ h}^{-1}$). On kaolinite, benoxacor degradation in mixtures (0.50 – 0.67 h^{-1}) was slightly slower than when it was irradiated alone ($0.72 \pm 0.01 \text{ h}^{-1}$). In contrast, on quartz, the rate constant of benoxacor decreased from 2.1 to 0.92 h^{-1} as its initial surface concentration increased from 4.8×10^{-4} to $8.3 \times 10^{-3} \mu\text{mol cm}^{-2}$. The time profile (SI Figure S2, frame B-2) showed no appreciable deviation from pseudo-first-order kinetics regardless of the initial surface concentration.

Because the relative concentrations of metolachlor and benoxacor in the mixtures covaried with benoxacor's initial surface concentration, further experiments were conducted on quartz for benoxacor alone with varying initial concentrations corresponding to those in the mixtures (Figure 2E). When benoxacor was irradiated alone, its degradation rate constant also generally decreased with increasing initial concentration, from $1.36 \pm 0.3 \text{ h}^{-1}$ at $4.8 \times 10^{-4} \mu\text{mol cm}^{-2}$ to $0.67 \pm 0.02 \text{ h}^{-1}$ at $1 \times 10^{-2} \mu\text{mol cm}^{-2}$. This may be attributed to the higher degree of molecular aggregation with higher initial surface concentrations, which reduces light exposure to the molecules in the interior of the aggregates and thereby attenuates photolysis. A previous study on the photolysis of 31 pesticides on glass also reported 31–71% decrease in the pseudo-first-order rate constants when the surface concentrations were increased 10-fold.⁵¹ The dependence of benoxacor photolysis rate on its initial surface concentration seems to contradict the pseudo-first-order kinetics shown in the degradation time profiles (i.e., benoxacor decay did not accelerate over time; Figure 2B and SI Figure S2). We posit that this was because of the sunlight screening effects of benoxacor's photoproducts; the benoxacor molecules in the interior of the aggregates did not receive more light as those on the exterior decayed. (Further discussion in SI Text S10. The sunlight absorption property of the photoproducts will be further discussed in Section 3.3.)

Figure 2E also shows that benoxacor degradation in mixtures on quartz was 1.5–2 times faster than when it was applied alone at the same initial concentration. The promotion of benoxacor decay by metolachlor is similar to that reported for the mixture of the herbicide cycloxydim and the fungicide chlorothalonil on paraffin wax: Chlorothalonil absorbs less sunlight than cycloxydim, but the presence of chlorothalonil ($5.6 \times 10^{-3} \mu\text{mol cm}^{-2}$, 1:1 molar ratio with cycloxydim) resulted in a 3-fold increase in cycloxydim degradation rate.²²

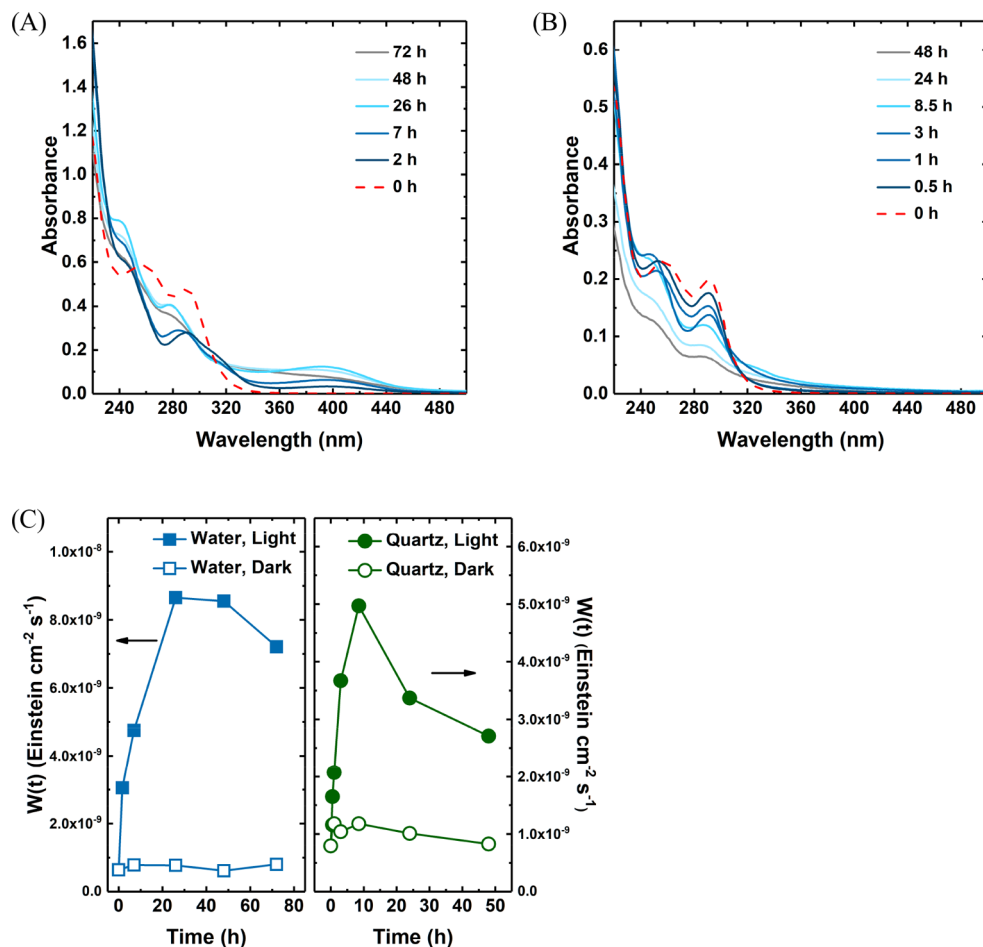


Figure 3. Absorption spectra of irradiated mixtures of benoxacor/metolachlor (A) in water and (B) on quartz. The initial benoxacor/metolachlor molar ratio was 10:1. (C) Sunlight absorption ability of the mixture as a function of irradiation time. Aqueous samples were directly analyzed. Surface samples were extracted by 5 mL acetonitrile and the extracts were analyzed.

This phenomenon was attributed to hydrogen atom transfer between triplet-state chlorothalonil and ground-state cycloxydim.^{22,52,53} Metolachlor conceivably could also form an excited triplet upon absorbing sunlight. Alternatively, the weakly absorbing metolachlor may act as a relatively inert component that increased the spacing between benoxacor molecules, exposing them to more incident light and promoting their direct photolysis. Further study is needed to investigate these phenomena.

3.3. Absorption Spectra and Photoproducts of Irradiated Benoxacor/Metolachlor Mixtures. The absorption spectra (220–500 nm) of the irradiated aqueous mixtures and of the acetonitrile extracts of quartz surface mixtures (benoxacor/metolachlor 10:1) are shown in Figure 3A and B, respectively. Over the course of the experiments, the signature absorption peaks of benoxacor (257 and 289 nm in water, and 257 and 293 nm in acetonitrile) diminished, but a change in the shape of the absorbance spectrum was also observed. Additionally, absorbance at wavelengths above 310 nm increased, indicating that photoproducts capable of absorbing sunlight were formed. Figure 3C shows the change in the sunlight absorption ability $W(t)$ of the mixtures with increasing irradiation time. Both in water and on quartz, there was initially a rapid increase in the sunlight absorption ability of the reaction mixtures concurrent with the decay of benoxacor. The sunlight absorption ability of the aqueous and quartz samples

peaked at 26 and 8.5 h, respectively, when it was 14- and 6-times higher than that of the original mixture. In water, the peak time (26 h) was much later than the time for benoxacor to reach 90% decay (1.5 h) (SI Figure S2, frame A-2); on quartz, the peak time (8.5 h) was the same as that for 90% benoxacor decay (SI Figure S2, frame B-2). These results suggest an accumulation of sunlight-absorbing products in the irradiated mixtures, consistent with the observation on quartz that sensitized metolachlor decay continued after complete removal of benoxacor. In water, despite the accumulation of sunlight-absorbing products, sensitized decay of metolachlor was ostensibly slow.

Figure 4 shows the 3D plots of the HPLC-DAD data sets for the irradiated samples from experiments in water and on quartz. The samples initially contained benoxacor alone or a 10:1 benoxacor/metolachlor mixture. In all reaction systems, product peaks were detected with retention times between 3.5 and 7 min, which were shorter than the retention times of benoxacor (7.3 min) and metolachlor (8.4 min), suggesting that the photoproducts featured more hydrophilic functional groups and/or were smaller than the parent compounds. Experiments using up to 90% acetonitrile as eluent did not yield additional product peaks with retention time longer than benoxacor or metolachlor. None of these product peaks were detected in the dark control samples (SI Figure S5C).

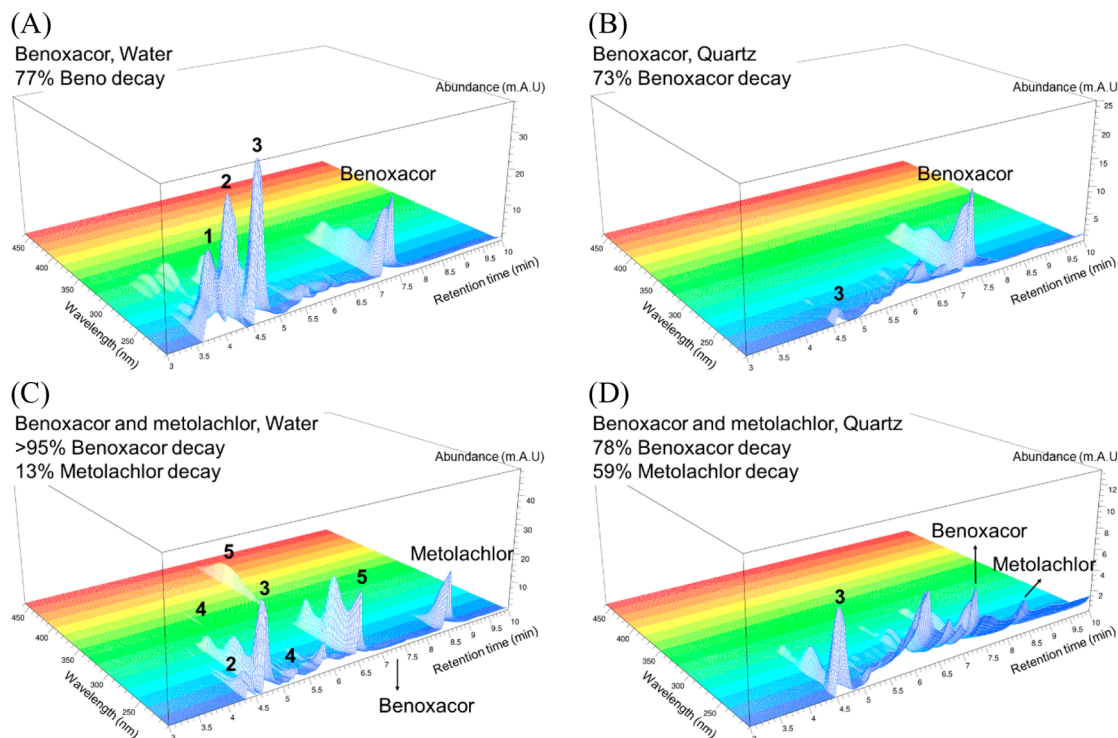


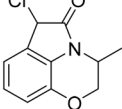
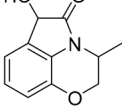
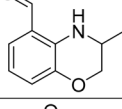
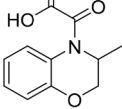
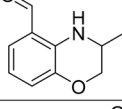
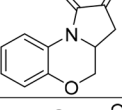
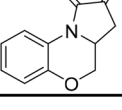
Figure 4. Three-dimensional plots of the HPLC-DAD data sets of irradiated benoxacor samples (A) in water and (B) on quartz, and irradiated mixtures (C) in water and (D) on quartz. Mixtures feature a 10:1 initial benoxacor/metolachlor molar ratio. The sampling time and corresponding parent compound decay are shown in [SI Table S5](#).

Among different samples, peaks with the same retention time and similar spectra were considered as the same product (or the same group of products). Five distinct product peaks were observed in the 3D plots, and their retention times are summarized in [SI Table S6](#). Fewer identifiable peaks were observed on quartz than in water. Peak 3 was detected in all samples; peaks 1 and 2 representing the most polar products were only detected in water but not on quartz. There were also unresolved peaks with retention times between 5 and 7 min in all samples. In water, peaks 4 and 5 were only detected in mixtures. The spectra of all five peaks showed absorption within the sunlight range (>290 nm), suggesting that they represent products contributing to the overall sunlight absorption ability of the samples. Peaks 4 and 5 have absorption bands with a maximum at 328 and 396 nm, respectively. During irradiation experiments in water, a yellow color gradually developed in the mixture samples over the course of 72 h, consistent with the formation of products absorbing light around 396 nm.

UPLC-qTOF analyses were conducted to further characterize the photoproducts. [Table 1](#) summarizes the five photoproducts identified; their mass spectra are shown in [SI Figure S6](#). [SI Figure S7](#) shows the chromatogram of the irradiated 10:1 benoxacor/metolachlor aqueous sample as an example. All five products have structures similar to benoxacor. These photoproducts are of comparable size as benoxacor, but have shorter retention time. A comparison of molecular structures between the putative products and benoxacor suggest that dechlorination may be one of the first steps for benoxacor photodegradation. In water, product I, with one remaining chlorine atom, was detected after 5 min irradiation of benoxacor, but was not detected after 1 h, suggesting that it was an intermediate. In water, product III was detected in both

benoxacor only and benoxacor/metolachlor mixture samples; products II and IV have similar retention times, but product II was only detected in the benoxacor sample, whereas product IV was only detected in the mixture. On quartz, a distinct product V was detected in both benoxacor and mixture samples, while products I–IV were not detected. All putative photoproducts retained conjugated moieties, which could explain the sunlight absorption ability of the irradiated samples. None of these photoproducts were detected in the time zero sample or the dark control samples. Because different columns and eluent gradients were used in the HPLC-DAD and UPLC-qTOF analyses, and because qTOF response depends on ionization efficiency while DAD does not, we did not attempt to correlate the peaks obtained from these two analyses. In this project, our sample analysis included UPLC-TOF-MS; MS/MS experiments were not conducted. Kral et al.³⁶ also conducted experiments to characterize the photoproducts of benoxacor in water via high-resolution mass spectrometry as well as nuclear magnetic resonance (NMR) spectroscopy, including two-dimensional NMR. Products I, II, and III that we observed from benoxacor photolysis in water when applied individually matched the corresponding products in Kral's study. These products correspond to Level 2b (probable structure by diagnostic evidence) of the confidence levels in high-resolution MS analysis proposed by Schymanski et al.⁵⁴ The two products unique to our investigation (IV and V) were postulated based on exact mass and UPLC retention time data (i.e., polarity relative to benoxacor). Due to the absence of corroborating MS/MS or NMR data, these structural assignments can be assigned Level 3 confidence (tentative candidates) based on the scale proposed by Schymanski et al.⁵⁴

Table 1. Photoproducts of Benoxacor and Benoxacor/Metolachlor Mixtures Characterized by UPLC-ESI(+)qTOF.^a

Sample	Reaction time (h)	Parent decay	#	RT (min)	Products	
					(M+H) ⁺ m/z (Da)	Putative Structure
Water	0.08	10%	I	1.26	measured: 224.0477 calculated: 224.0473 difference: 1.8 ppm	
	1	77%	II	0.43	measured: 206.0819 calculated: 206.0812 difference: 3.4 ppm	
			III	1.55	measured: 178.0870 calculated: 178.0863 difference: 3.9 ppm	
Benoxacor + Metolachlor Mixture	1.5	Benoxacor 90% Metolachlor 0%	IV	0.43	measured: 222.0790 calculated: 222.0761 difference: 13 ppm	
			III	1.52	measured: 178.0887 calculated: 178.0863 difference: 13 ppm	
	5	87%	V	0.63	measured: 204.0661 calculated: 204.0655 difference: 2.9 ppm	
Quartz	1	Benoxacor 59% Metolachlor 49%	V	0.64	measured: 204.0672 calculated: 204.0655 difference: 8.3 ppm	

^aThe initial concentrations of metolachlor and benoxacor are shown in SI Tables S1 and S2. Product identification was based on measurements of exact masses. RT = retention time; *m/z* = mass-to-charge ratio; *m/z* difference = $\frac{\text{measured } m/z - \text{calculated } m/z}{\text{calculated } m/z} \times 10^6$.

4. ENVIRONMENTAL SIGNIFICANCE

We evaluated the sunlight photolysis of the herbicide metolachlor and the safener benoxacor (individually and as mixtures) in water and on quartz and kaolinite surfaces. Although considered an “inert” ingredient in the formulations, benoxacor exhibited complex photochemical behavior. Using results from the kaolinite experiments (Figure 1C), the direct photolysis half-lives of metolachlor and benoxacor on soil were estimated to be 4.7 days and 2.9 h, respectively, based on the sunlight intensity for a midsummer day at 40°N latitude (sea level) under clear skies and accounting for diurnal variation.^{55,56} The identified photoproducts of benoxacor shared structural similarity to the parent compound, suggesting that their ecotoxicity and transformation processes, in addition to those of benoxacor, should be considered in future environmental fate studies.

This research is one of the few attempts to investigate the photochemical behavior of commercial agrochemical mixtures on surfaces. At the field-relevant benoxacor/metolachlor ratio (0.1:1), the presence of benoxacor accelerated metolachlor degradation on quartz by 2-fold; both benoxacor and its photoproducts acted as photosensitizers. It should be noted that field application of benoxacor and metolachlor typically uses higher surface concentrations than this study, which can

lead to a higher probability for benoxacor and its photoproducts to sensitize metolachlor degradation. On the other hand, it should be acknowledged that soil is a heterogeneous system containing domains of clay minerals and organic matter.⁴ Metolachlor ($\log K_{ow} = 2.90$)⁵⁷ and benoxacor ($\log K_{ow} = 2.79$),⁵⁷ both being nonionic compounds, are likely to partition into the organic matter phase. We expect the close proximity of benoxacor and metolachlor to facilitate similar interactions as observed on quartz. Future studies should evaluate the roles of soil organic matter in benoxacor-sensitized metolachlor degradation, considering the partitioning behavior of the agrochemicals as well as the potential scavenging and sensitizing effects of organic matter.

Our results also showed that photochemical reactions on surfaces can be distinct from those in water in terms of rates and products. The benoxacor-sensitized metolachlor degradation was much more pronounced on quartz than in water. The photoproduct of benoxacor identified from quartz samples was not detected in aqueous samples. Overall, our findings suggest that the environmental fate models for agrochemicals should consider the interaction between active ingredients and other constituents in the commercial formulations, especially for their photolysis on environmental surfaces.

ASSOCIATED CONTENT

Supporting Information

The Supporting Information is available free of charge on the ACS Publications website at DOI: [10.1021/acs.est.9b01243](https://doi.org/10.1021/acs.est.9b01243).

Texts, tables, and figures on chemicals, experimental procedures, analytical methods, quantum yield calculation, standard error calculation, and additional discussion on the loss of parent compounds in dark control experiments and benoxacor degradation kinetics ([PDF](#))

AUTHOR INFORMATION

Corresponding Author

*Phone: (716) 645-4015; fax: (716) 645-3667; email: ningdai@buffalo.edu.

ORCID

Ning Dai: [0000-0002-8468-5611](https://orcid.org/0000-0002-8468-5611)

Notes

The authors declare no competing financial interest.

ACKNOWLEDGMENTS

This research was supported by the National Science Foundation (NSF, Nos. 1610807, 1531562, and 1703796). Leandra Caywood was supported through an NSF-funded REU program (No. EEC-1559989).

REFERENCES

- 1) Remucal, C. K. The role of indirect photochemical degradation in the environmental fate of pesticides: a review. *Environ. Sci.: Processes Impacts* **2014**, *16* (4), 628–653.
- 2) Burrows, H. D.; Canle, L. M.; Santaballa, J. A.; Steenken, S. Reaction pathways and mechanisms of photodegradation of pesticides. *J. Photochem. Photobiol., B* **2002**, *67* (2), 71–108.
- 3) Zeng, T.; Arnold, W. A. Pesticide photolysis in prairie potholes: probing photosensitized processes. *Environ. Sci. Technol.* **2013**, *47* (13), 6735–6745.
- 4) Katagi, T. Photodegradation of pesticides on plant and soil surfaces. *Rev. Environ. Contam. Toxicol.* **2004**, *182*, 1–189.
- 5) Vasquez, M.; Cahill, T.; Tjeerdema, R. Soil and glass surface photodegradation of etofenprox under simulated California rice growing conditions. *J. Agric. Food Chem.* **2011**, *59* (14), 7874–7881.
- 6) Suzuki, Y.; Lopez, A.; Ponte, M.; Fujisawa, T.; Ruzo, L. O.; Katagi, T. Photoinduced oxidation of the insecticide phenothrin on soil surfaces. *J. Agric. Food Chem.* **2011**, *59* (18), 10182–10190.
- 7) Frank, M. P.; Graebing, P.; Chib, J. Effect of soil moisture and sample depth on pesticide photolysis. *J. Agric. Food Chem.* **2002**, *50* (9), 2607–2614.
- 8) Mountacer, H.; Atifi, A.; Wong-Wah-Chung, P.; Sarakha, M. Degradation of the pesticide carbofuran on clay and soil surfaces upon sunlight exposure. *Environ. Sci. Pollut. Res.* **2014**, *21* (5), 3443–3451.
- 9) Hebert, V. R.; Miller, G. C. Depth dependence of direct and indirect photolysis on soil surfaces. *J. Agric. Food Chem.* **1990**, *38* (3), 913–918.
- 10) Werner, J. J.; McNeill, K.; Arnold, W. A. Photolysis of chlortetracycline on a clay surface. *J. Agric. Food Chem.* **2009**, *57* (15), 6932–6937.
- 11) Ciani, A.; Goss, K. U.; Schwarzenbach, R. P. Light penetration in soil and particulate minerals. *Eur. J. Soil Sci.* **2005**, *56* (5), 561–574.
- 12) Helz, G. R.; Zepp, R. G.; Crosby, D. G. *Aquatic and Surface Photochemistry*; CRC Press, Taylor & Francis Group, 1994.
- 13) Menager, M.; Sarakha, M. Simulated solar light photo-transformation of organophosphorus azinphos methyl at the surface of clays and goethite. *Environ. Sci. Technol.* **2013**, *47* (2), 765–772.
- 14) Mazellier, P.; Sulzberger, B. Diuron degradation in irradiated, heterogeneous iron/oxalate systems: the rate-determining step. *Environ. Sci. Technol.* **2001**, *35* (16), 3314–3320.
- 15) Konstantinou, I. K.; Zarkadis, A. K.; Albanis, T. A. Photodegradation of selected herbicides in various natural waters and soils under environmental conditions. *J. Environ. Qual.* **2001**, *30* (1), 121–130.
- 16) Siampiringue, M.; Wong Wah Chung, P.; Koriko, M.; Tchangbedji, G.; Sarakha, M. Clay and soil photolysis of the pesticides mesotrione and metsulfuron methyl. *Appl. Environ. Soil Sci.* **2014**, *2014*, 1–8.
- 17) Gohre, K.; Miller, G. C. Singlet oxygen generation on soil surfaces. *J. Agric. Food Chem.* **1983**, *31* (5), 1104–1108.
- 18) Gohre, K.; Scholl, R.; Miller, G. C. Singlet oxygen reactions on irradiated soil surfaces. *Environ. Sci. Technol.* **1986**, *20* (9), 934–8.
- 19) Clements, P.; Wells, C. H. Soil sensitised generation of singlet oxygen in the photodegradation of bioresmethrin. *Pestic. Sci.* **1992**, *34* (2), 163–166.
- 20) Hazen, J. L. Adjuvants—terminology, classification, and chemistry. *Weed Technol.* **2000**, *14* (4), 773–784.
- 21) ter Halle, A.; Lavieille, D.; Richard, C. The effect of mixing two herbicides mesotrione and nicosulfuron on their photochemical reactivity on cuticular wax film. *Chemosphere* **2010**, *79* (4), 482–487.
- 22) Monadjemi, S.; ter Halle, A.; Richard, C. Accelerated dissipation of the herbicide cycloxydim on wax films in the presence of the fungicide chlorothalonil and under the action of solar light. *J. Agric. Food Chem.* **2014**, *62* (21), 4846–4851.
- 23) Eyheraguibel, B.; Richard, C.; Ledoigt, G.; Ter Halle, A. Photoprotection by plant extracts: A new ecological means to reduce pesticide photodegradation. *J. Agric. Food Chem.* **2010**, *58* (17), 9692–9696.
- 24) Davies, J.; Caseley, J. C. Herbicide safeners: a review. *Pestic. Sci.* **1999**, *55* (11), 1043–1058.
- 25) Atwood, D.; Paisley-Jones, C. *Pesticides Industry Sales and Usage 2008–2012 Market Estimates*, Google Scholar; U.S. Environmental Protection Agency: Washington, DC, 2017.
- 26) Foy, C. L. Progress and developments in adjuvant use since 1989 in the USA. *Pestic. Sci.* **1993**, *38* (2–3), 65–76.
- 27) Sivey, J. D.; Lehmler, H.-J.; Salice, C. J.; Ricko, A. N.; Cwiertny, D. M. Environmental fate and effects of dichloroacetamide herbicide safeners: “Inert” yet biologically active agrochemical ingredients. *Environ. Sci. Technol. Lett.* **2015**, *2* (10), 260–269.
- 28) Safety Data Sheet: Dual II Magnum®. <http://www.syngentacropprotection.com/pdf/msds/dual%20ii%20a9558c%2002042015.pdf> (accessed October 18, 2018).
- 29) Worthing, C.; Walker, S. *The Pesticide Manual: A World Compendium*. British Crop Protection Council; Thornton Heath. In UK, 1987.
- 30) Hoagland, R. E.; Zablotowicz, R. M.; Locke, M. A. *An Integrated Phytoremediation Strategy for Chloroacetamide Herbicides in soil*, 1997.
- 31) DUAL® II MAGNUM ® Herbicide. http://www2.dupont.com/Crop_Protection/en_CA/assets/downloads/20100224_DUAL%20II%20Magnum.pdf (accessed October 18, 2018).
- 32) Jablonkai, I. Herbicide safeners: effective tools to improve herbicide selectivity. In *Herbicides-Current Research and Case Studies in Use*; InTech, 2013.
- 33) Müller, M. D.; Poiger, T.; Buser, H.-R. Isolation and identification of the metolachlor stereoisomers using high-performance liquid chromatography, polarimetric measurements, and enantioselective gas chromatography. *J. Agric. Food Chem.* **2001**, *49* (1), 42–49.
- 34) Dimou, A. D.; Sakkas, V. A.; Albanis, T. A. Metolachlor photodegradation study in aqueous media under natural and simulated solar irradiation. *J. Agric. Food Chem.* **2005**, *53* (3), 694–701.
- 35) Wilson, R. I.; Mabury, S. A. Photodegradation of metolachlor: isolation, identification, and quantification of monochloroacetic acid. *J. Agric. Food Chem.* **2000**, *48* (3), 944–950.

- (36) Kral, A. E.; Pflug, N. C.; McFadden, M.; LeFevre, G. H.; Sivey, J. D.; Cwiertny, D. M. Photochemical transformations of dichloroacetamide safeners. *Environ. Sci. Technol.*, **2019**, DOI: 10.1021/acs.est.9b00861.
- (37) Abu-Qare, A. W.; Duncan, H. J. Photodegradation of the herbicide EPTC and the safener dichlormid, alone and in combination. *Chemosphere* **2002**, *46* (8), 1183–1189.
- (38) Su, L.; Sivey, J. D.; Dai, N. Emerging investigator series: sunlight photolysis of 2,4-D herbicides in systems simulating leaf surfaces. *Environ. Sci.: Processes Impacts* **2018**, *20* (8), 1123–1135.
- (39) Woodward, E. E.; Hladik, M. L.; Kolpin, D. W. Occurrence of dichloroacetamide herbicide safeners and co-applied herbicides in midwestern US streams. *Environ. Sci. Technol. Lett.* **2018**, *5* (1), 3–8.
- (40) Ciani, A.; Goss, K.-U.; Schwarzenbach, R. P. Photodegradation of organic compounds adsorbed in porous mineral layers: Determination of quantum yields. *Environ. Sci. Technol.* **2005**, *39* (17), 6712–6720.
- (41) Balmer, M. E.; Goss, K.-U.; Schwarzenbach, R. P. Photolytic transformation of organic pollutants on soil surfaces an experimental approach. *Environ. Sci. Technol.* **2000**, *34* (7), 1240–1245.
- (42) Ciani, A.; Goss, K.-U.; Schwarzenbach, R. P. *J. C. Chemosphere* **2005**, *61* (10), 1410–1418.
- (43) Corrochano, P.; Nachtigalova, D.; Kla'n, P. Photooxidation of aniline derivatives can be activated by freezing their aqueous solutions. *Environ. Sci. Technol.* **2017**, *51* (23), 13763–13770.
- (44) Mizuguchi, J.; Senju, T. Solution and solid-state spectra of quinacridone derivatives as viewed from the intermolecular hydrogen bond. *J. Phys. Chem. B* **2006**, *110* (39), 19154–19161.
- (45) Wardle, B. *Principles and Applications of Photochemistry*; John Wiley & Sons, 2009.
- (46) Module 2: Soil-Water-Contaminant Interaction. <https://nptel.ac.in/courses/105103025/module2/lec4/3.html> (accessed February 18, 2019).
- (47) Bower, J. P.; Anastasio, C. Degradation of organic pollutants in/on snow and ice by singlet molecular oxygen (${}^1\text{O}_2{}^*$) and an organic triplet excited state. *Environ. Sci.: Processes Impacts* **2014**, *16* (4), 748–756.
- (48) Chen, Z.; Anastasio, C. Concentrations of a triplet excited state are enhanced in illuminated ice. *Environ. Sci.: Processes Impacts* **2017**, *19* (1), 12–21.
- (49) Gligorovski, S.; Strekowski, R.; Barbat, S.; Vione, D. Environmental implications of hydroxyl radicals ($\bullet\text{OH}$). *Chem. Rev.* **2015**, *115* (24), 13051–13092.
- (50) Kanazawa, S.; Kawano, H.; Watanabe, S.; Furuki, T.; Akamine, S.; Ichiki, R.; Ohkubo, T.; Kocik, M.; Mizeraczyk, J. Observation of OH radicals produced by pulsed discharges on the surface of a liquid. *Plasma Sources Sci. Technol.* **2011**, *20* (3), 034010.
- (51) Chen, Z.; Zabik, M. J.; Leavitt, R. A. Comparative study of thin film photodegradative rates for 36 pesticides. *Ind. Eng. Chem. Prod. Res. Dev.* **1984**, *23* (1), 5–11.
- (52) Yuan, Q.; Toroz, D.; Kidley, N.; Gould, I. R. Mechanism of photoinduced triplet intermolecular hydrogen transfer between cycloxydim and chlorothalonil. *J. Phys. Chem. A* **2018**, *122* (17), 4285–4293.
- (53) Monadjemi, S.; El Roz, M.; Richard, C.; Ter Halle, A. Photoreduction of chlorothalonil fungicide on plant leaf models. *Environ. Sci. Technol.* **2011**, *45* (22), 9582–9589.
- (54) Schymanski, E. L.; Jeon, J.; Gulde, R.; Fenner, K.; Ruff, M.; Singer, H. P.; Hollender, J. *Identifying Small Molecules via High Resolution Mass Spectrometry: Communicating Confidence*; ACS Publications, 2014.
- (55) Schwarzenbach, R. P.; Gschwend, P. M.; Imboden, D. M. *Environmental Organic Chemistry*, 2nd ed.; Wiley: Hoboken, NJ, 2003; p xiii, 1313.
- (56) McConville, M. B.; Cohen, N. M.; Nowicki, S. M.; Lantz, S. R.; Hixson, J. L.; Ward, A. S.; Remucal, C. K. A field analysis of lampicide photodegradation in Great Lakes tributaries. *Environ. Sci.: Processes Impacts* **2017**, *19* (7), 891–900.
- (57) U.S. Environmental Protection Agency. *Estimation Programs Interface Suite for Microsoft Windows*, 2014.